Improved Photoluminescence of MnS/ZnS Core/Shell Nanocrystals by Controlling Diffusion of Mn Ions into the ZnS Shell

Jinju Zheng,[†,‡] Wenyu Ji,[†] Xiuying Wang,[†] Micho Ikezawa,[§] Pengtao Jing,[†,‡] Xueyan Liu,[†] Haibo Li,[||] Jialong Zhao,*[,†] and Yasuaki Masumoto*[,§]

Key Laboratory of Excited State Processes, Changchun Institute of Optics, Fine Mechanics and Physics, Chinese Academy of Sciences, 3888 Eastern South Lake Road, Changchun 130033, China, Graduate School of Chinese Academy of Sciences, Beijing 100039, China, Institute of Physics, University of Tsukuba, Tsukuba, Ibaraki 305-8571, Japan, and Institute of Condensed Matter Physics and Materials Science, Jilin Normal University, Siping 136000, China

Received: May 18, 2010; Revised Manuscript Received: August 5, 2010

We studied the diffusion of Mn ions in MnS/ZnS core/shell nanocrystals (NCs) from the MnS core to the ZnS shell by steady-state and time-resolved photoluminescence (PL) spectroscopy. The colloidal MnS/ZnS core/shell NCs with different thicknesses of the ZnS shell synthesized in octadecene with nucleation doping strategy were annealed at different temperatures. It was found that the PL intensity and lifetime of the MnS/ZnS NCs with a thin ZnS shell significantly decreased with increasing annealing time in the heat treatment temperature range of 220−300 °C, resulting from the diffusion of Mn ions in the MnS/ZnS core/shell NCs to the surface of the ZnS shell, while the PL intensity and lifetime of the NCs with a thick ZnS shell remained almost constant in the temperature range. Furthermore, it was noted that the MnS/ZnS NCs with a small MnS core of about 2.0 nm in diameter exhibited high PL quantum yield of greater than 40%. The experimental results indicated that highly efficient luminescent Mn-doped ZnS NCs could be obtained by controlling the diffusion of Mn ions into the ZnS shell via annealing the core/shell NCs and using small-sized MnS cores and by optimizing the thickness of the ZnS passivating layer.

Introduction

Transition-metal Mn ion-doped semiconductor nanocrystal (NC) emitters have been widely investigated in view of their optical properties such as long photoluminescence (PL) lifetime, high PL quantum yield (QY), and minimized self-absorption and applications as a light-emitting source in optoelectronic devices and in bioimaging.[1−17] Especially for ZnS:Mn NCs, they are a greener material that is free from both Cd and Se, and popular nanophosphors for electroluminescent devices.[8−10] Despite systematic efforts, which began in 1994, to introduce intentional impurities into NCs,[1] when ZnS NCs were first doped with Mn impurities, there has been little progress in optimizing the PL QY of Mn ions from dispersed colloidal Mn-doped ZnS NCs due to the lack of the ability to precisely control the doping of semiconductor NCs.[1−7] This situation was substantially improved by Peng's group with the development of a new doping strategy, nucleation doping;[12−14] for example, Mn-doped ZnSe NCs prepared by growing a ZnSe shell on the MnSe core exhibited PL QY up to 50% and good thermal stability.[13,14] This method, allows one to place dopants at the desired initial positions in the host NCs, is expected to significantly improve the PL QY of the doped NCs by controlling the diffusion of Mn ions in the NCs and the structure of NCs.

Recently, we reported efficient PL of Mn ions from the MnS/ZnS core/shell NCs with a PL QY of 35% synthesized by the nucleation doping strategy.[17] The PL of Mn ions is currently considered to come from the energy transfer from photoexcited ZnS shells to the Mn ions in a diffusion layer at the interface between the MnS core and the pure ZnS overcoating layer.[17] Therefore, the PL QY of the NCs should be greatly influenced by structural properties of the Mn ion diffusion layer, which is directly determined by the diffusion of Mn ions into the ZnS shell during the colloidal growth process.[13,14,17] The diffusion of Mn ions in II−VI semiconductors has been extensively studied.[18−20] Some researchers reported the diffusion rate of Mn ions in bulk CdTe at the temperature of 300 °C is only 0.1−0.3 nm/h.[18] This means that the diffusion of Mn ions in II−VI semiconductor NCs should be negligible during colloidal growth in the temperature range below 300 °C. However, for the MnS/ZnS (or MnSe/ZnSe) NCs synthesized by nucleation doping strategy, the presence of the Mn ion PL, which was considered to come from the Mn ions in a diffusion layer, obviously indicated that the Mn ions had diffused from the MnS (MnSe) core into the ZnS (ZnSe) shell during the growth process.[13,14,17] Further study indicated that the critical temperature for "lattice diffusion" in NCs was substantially lower than that in the bulk crystals.[20] To improve the PL QY of the MnS/ZnS NCs synthesized by nucleation doping strategy, it is necessary to understand the diffusion process of Mn ions in the NCs on their PL properties in detail.

In this work, we report the study of the diffusion process of Mn ions in MnS/ZnS NCs from the MnS core into the ZnS shell by steady-state and time-resolved PL spectroscopy. The MnS/ZnS core/shell NCs with different MnS core size and ZnS shell thickness synthesized by nucleation doping strategy were annealed in original solution in the heat treatment temperature range of 220−300 °C. The quenching of the Mn ion PL intensity

* To whom correspondence should be addressed. J.Z.: phone, +86-431-86176029; e-mail, zhaojl@ciomp.ac.cn. Y.M.: phone, +81-29-8534248; e-mail, shoichi@sakura.cc.tsukuba.ac.jp.
[†] Chinese Academy of Sciences.
[‡] Graduate School of Chinese Academy of Sciences.
[§] University of Tsukuba.
[||] Jilin Normal University.

10.1021/jp104513k
Published on Web 08/24/2010

combining with the shortening of its lifetime with increasing annealing temperature and time was explained in terms of the diffusion of Mn ions from the MnS core toward the surface of the ZnS shell. We will discuss the diffusion process of Mn ions into the ZnS shell during the colloidal growth of MnS/ZnS core/shell NCs based on PL spectroscopy to explore the formation of highly efficient luminescent Mn-doped ZnS NCs.

Experimental Section

In this experiment, MnS/ZnS core/shell NCs were synthesized by nucleation doping strategy that was published previously.[17]

(a) Preparation of stock solutions occurred as follows: Octadecene sulfur (ODES) solution was prepared by adding 0.039 g of S and 0.4 g of octadecylamine (ODA) into 3 mL of octadecene (ODE). The zinc precursor solutions were prepared by dissolving 0.7 g of $ZnSt_2$ into 6.5 mL of ODE with heating under argon; the concentration of $ZnSt_2$ was 0.1 g/mL.

(b) Samples with different shell thicknesses, referred to as A, B, and C, were synthesized to study the diffusion of Mn ions in MnS/ZnS core/shell NCs. For a typical synthesis of MnS/ZnS NCs, 12 mL of ODE and 0.03 g of $MnSt_2$ were loaded into a 50 mL three-necked flask and degassed at 110 °C for 15 min by bubbling with argon. The temperature was then raised to 270 °C. In a separate vial, 3 mL of ODES solution was heated until the solution turned colorless and then was swiftly injected into the reaction flask at 270 °C. The reaction temperature was swiftly cooled to 170 °C and then increased to 250 °C for ZnS overcoating. The zinc precursor solution (1.5 mL) was added dropwise into the reaction flask at 250 °C and maintained at that temperature for 10 min, the obtained nanocrystals referred to as sample A. To obtain sample B, the additional $ZnSt_2$ solution (1.5 mL) was injected at 250 °C with 10 min intervals. For sample C, the total amount of $ZnSt_2$ solution was 5 mL; after the first overcoating, the remaining $ZnSt_2$ solution was injected by adding 1.75 mL after 10 min intervals two times. After the reaction finished, the temperature of the solution was cooled down to room temperature and then increased to the needed temperature for further thermal treatment without any purification procedure. Small aliquots were removed from the reaction solution with a syringe during annealing to monitor the evolution of the PL properties. Because PL intensity varied somewhat for the different purification procedure, the aliquots dispersed in $CHCl_3$ directly without purification procedure were used to measure absorption, excitation, and PL spectra as well as PL decays.

(c) Samples D, E, and F were synthesized to study the effect of the growth temperature for the first overcoating ZnS layer on the PL QY of the NCs. After the injection of ODES stock solution into the reaction flask at 270 °C, the reaction temperature was swiftly cooled to 170 °C and then increased to 200 °C (sample D), 250 °C (sample E), or 280 °C (sample F) with steps of 15 °C/min for ZnS overcoating; the $ZnSt_2$ solution (1.0 mL) was added into the reaction flask and the reaction temperature then was set at 280 °C and maintained at that temperature for 20 min for Mn ion diffusion. The additional $ZnSt_2$ solution (6 mL) was injected by adding 3 mL after 15 min intervals two times at 250 °C. Finally, the reaction temperature was cooled to room temperature, and the NCs were precipitated using acetone. High-quality MnS/ZnS NCs formed with small-sized MnS cores overcoated at low temperature were reproducible, demonstrating PL QYs of 40−50%.

X-ray diffraction (XRD) data were collected on a Rigaku XRD spectrometer with a Cu Kα line of 0.15418 nm for the purified MnS/ZnS core/shell NCs. The morphology of the NC samples was characterized by a transmission electron microscope (TEM) (TECNAI G2). The absorption spectra were recorded on a UV-3101PC UV−vis−NIR scanning spectrophotometer (Shimadzu). PL and excitation (PLE) spectra were recorded by a Hitachi F-4500 spectrophotometer. In the measurements of fluorescence dynamics, a 266 nm laser combined with a fourth harmonic generator was used as an excitation light. A Spex 1403 spectrometer and a boxcar integrator were used to record the fluorescence dynamics. All measurements were carried out at room temperature.

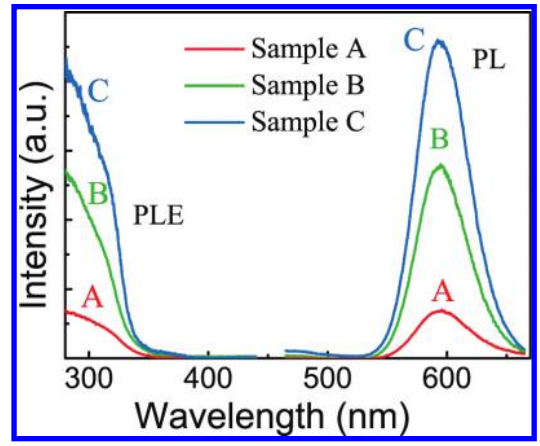

Figure 1. PL and PLE spectra of MnS/ZnS core/shell NCs with shell thicknesses of 2.2 (A: red lines), 3.7 (B: green lines), and 5.0 MLs (C: blue lines).

Results and Discussion

Figure 1 shows PL and PLE spectra of MnS/ZnS core/shell NCs with different ZnS shell thicknesses. As seen in Figure 1, a strong 595 nm Mn ion PL band with a full-width at half-maximum (fwhm) of about 50 nm and a large Stokes shift of about 270 nm comes from $^4T_1$ to $^6A_1$ transition from Mn ions in the ZnS lattice.[1−7,13−17] The PLE spectra of the orange emission in the MnS/ZnS core/shell NCs are also consistent with the absorption onset of the ZnS shells, indicating energy transfer from the photoexcited ZnS shells to the Mn ions.[17] The PL QY of the MnS/ZnS core/shell NCs increases from 4% to 23% when ZnS shells with 2.2, 3.7, and 5.0 monolayers (MLs) estimated in the following are grown on the MnS core, similar to previous experimental results.[17]

The XRD patterns of the MnS cores and MnS/ZnS core/shell NCs with different shell thicknesses are shown in Figure 2. For MnS cores, three obvious diffraction peaks located at 27.4°, 45.6°, and 54.0° correspond to the (111), (220), and (311) planes of zinc blende phase MnS, respectively (JCPDS No. 40-1288). These peaks shift to the standard position of zinc blende ZnS (JCPDS No. 05-0566) when a ZnS shell with varying thickness is grown onto the MnS core. However, the XRD patterns cannot provide any information about the diffusion process of the Mn ions from the MnS core into the ZnS shell during the colloidal growth of MnS/ZnS core/shell NCs.

Figure 3 shows the TEM images of the MnS core and MnS/ZnS core/shell NCs. As seen in Figure 3 (top), the NCs are nearly monodispersed. The sizes of MnS cores and MnS/ZnS core/shell NCs in samples A, B, and C were estimated to be 3.0, 4.2, 5.0, and 5.7 nm, respectively. On the basis of the thickness of 0.27 nm for a 1 ML ZnS shell with cubic structure,[21] the thicknesses of the ZnS overcoating layers for samples A, B, and C were estimated to be about 2.2, 3.7, and 5.0 MLs, respectively. It is well-known that heating NCs in solution may

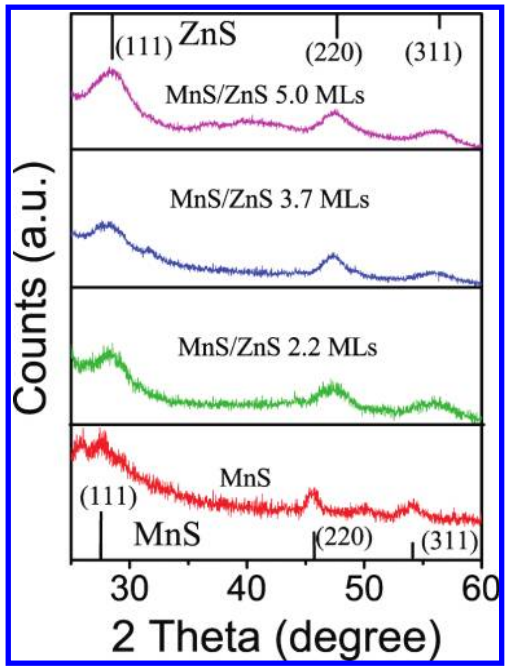

Figure 2. XRD patterns of MnS cores and MnS/ZnS core−shell NCs with different shell thicknesses.

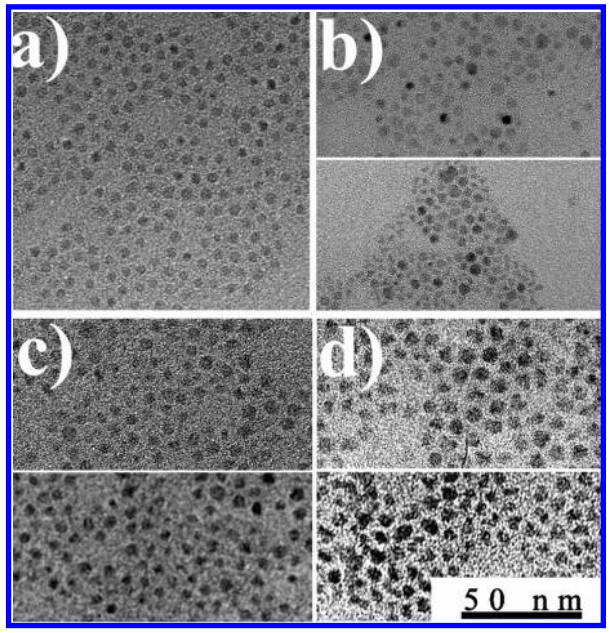

Figure 3. TEM images of 3.0 nm MnS core (a), and samples A (b), B (c), and C (d) MnS/ZnS core−shell NCs before (top) and after (bottom) heat treatment at 280 °C for 140 min, respectively.

cause NC Ostwald ripening, combining with the change of the shape and size distribution of the NCs.[22] It is not possible to study the diffusion process of Mn ions in the MnS/ZnS presynthesized NCs if the NCs go for Ostwald ripening during the annealing process. Fortunately, the TEM images of the NCs as seen in the bottom of Figure 3b−d confirm that the shape and size distribution of the NCs hardly change after the heat treatment, indicating no substantial ripening occurs during the heat treatment even at 280 °C for 140 min. This may be because the starting host particles are core/shell NCs, which are more stable than the pure core[20] and the reactant concentrations of sulfur and the ligand concentration of ODA in the growth solution are maintained sufficiently high through the entire annealing process.[23]

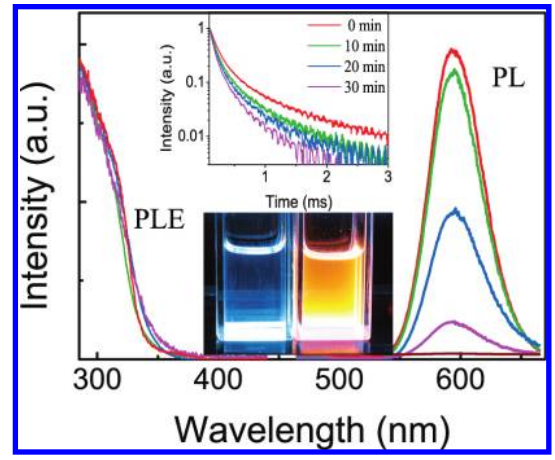

Figure 4. PL and PLE spectra of MnS/ZnS NCs with a thin shell of 2.2 MLs at an annealing temperature of 280 °C for different annealing times. The inset (top) shows PL decay curves of Mn ions in the NCs. The annealing times are 0 min (red lines), 10 min (green lines), 20 min (blue lines), 30 min (magenta lines), and 40 min (wine lines), respectively. The digital pictures in the inset (bottom) show the PL recovery for the MnS/ZnS QDs with a 2.2 ML ZnS shell before (left) and after (right) add the zinc precursor solution as discussed in this article.

The PLE and PL spectra of MnS/ZnS NCs with a shell thickness of 2.2 MLs annealed at a temperature of 280 °C for different times are shown in Figure 4. The onset and contour of their PLE spectra for the orange emission are hardly changed, suggesting the invariability of the NC size and distribution during the annealing process,[17] which is clearly confirmed by the TEM images. However, the orange PL intensity of Mn ions monotonously decreased with increasing annealing time during the heat treatment, and then completely quenched when the sample was annealed at 280 °C for about 40 min. We consider three possible explanations of the PL quenching: (i) The removal of ligands from the surface of the NCs. It is well-known that the decrease of the ligands on the surface of the NCs will result in formation of a large amount of surface dangling bonds, thus quenching the PL.[24,25] To test this, more ODA (0.2 g) was added into the solution that had been annealed at 280 °C for 40 min. The Mn ion PL intensity does not show any recovery. This means that the decrease in the PL intensity cannot be explained by the removal of the ligands on the surface of the NCs.[24] (ii) The Mn−Mn interaction in the NCs. Because the core is a pure MnS cluster, more Mn ions may diffuse into the interface layer during the annealing process, resulting in Mn−Mn interactions due to high Mn ion concentration. Such interactions will cause a reduction in the Mn ion PL QY.[26] However, the possibility can be eliminated by other experiments as discussed in the following. (iii) The diffusion of Mn ions in MnS/ZnS NCs from the MnS core to the NC surface. As discussed in our previous work, under the condition of steady-state excitation,[17,27] the PL QY of Mn ions, QY^{Mn}, the efficiency of the energy transfer from the QDs to Mn ions, Φ_{ET}, and the efficiency of the Mn ion emission, Φ_{Mn}, can be expressed by an equation $QY^{Mn} = \Phi_{ET}\Phi_{Mn}$. Therefore, the Mn ion PL QY is not only proportional to the efficiency of the Mn ion emission (Φ_{Mn}) but also to the efficiency of energy transfer (Φ_{ET}) from an exciton inside the ZnS shell to Mn ions. Considering that, the change of Φ_{ET} before and after annealing can be ignored due to the unchanged size distribution and the surface characteristics of the NCs,[5,27] while the Φ_{Mn} is directly influenced by the nonradiative relaxation rate from the Mn ions to the quenching centers.[27] The diffusion of Mn ions from the MnS core to the surface of the MnS/ZnS

NCs will result in the increase of the nonradiative relaxation rate from the Mn ions to the quenching centers, thus quenching the PL. Therefore, the decrease in the PL intensity during annealing is most likely to result from the diffusion of Mn ions to the NC surface. A similar result was also reported by Peng[20] who argued that impurities could efficiently diffuse to the NC surface at certain high temperatures, causing a decrease in the PL intensity of MnSe/ZnSe NCs.

One may argue that the decrease of the PL QY was due to the loss of the Mn ions of the NCs through "lattice ejection" during the annealing process at high temperature, which was proposed by Peng and co-workers.[15,20] At this moment, it is impossible to completely exclude this possibility in our case. However, we performed the reaction by adding additional precursors (1.5 mL of zinc precursor solution) into the annealed solution for further overcoating of the ZnS shell on the NCs. It was found that the PL intensity immediately obviously recovered as shown in the inset of Figure 4 and was even stronger than that of sample B. This means that the decrease of the PL intensity cannot be completely explained by the loss of the Mn ions and the Mn−Mn interactions in the NCs mentioned above. Therefore, annealing the NC sample at a suitable stage will benefit the efficient diffusion of Mn ions into the ZnS shell, resulting in higher PL QY for the core/shell NCs with an optimized ZnS passivating layer.

Ideally, if the Mn ions in MnS/ZnS NCs diffuse from the MnS core to the NC surface, this will consequently shorten the PL lifetime of Mn ions in the NCs due to the increase of the nonradiative relaxation rate from the Mn ions to the quenching centers.[17,27] The results shown in Figure 4 (inset) indicate that the PL lifetime of Mn ions in the NCs does monotonously decrease during the annealing process. The curves are fit by a function $I(t) = y_0 + A_1 \exp(-t/\tau_1) + A_2 \exp(-t/\tau_2) + A_3 \exp(-t/\tau_3)$,[17] where τ_1, τ_2, and τ_3 are the time constants and A_1, A_2, and A_3 are the normalized amplitudes of the components. The time constant of the isolated Mn ion PL in the MnS/ZnS NCs decreases monotonously from 1.35 to 0.68 ms with increasing annealing time, which is much shorter than the 1.8 ms PL lifetime of the typical single internal Mn ions,[28,29] indicating some Mn ions have diffused to the surface of the NCs during the overcoating and annealing process.[17,28,29] Therefore, the decrease in PL intensity and lifetime of Mn ions in MnS/ZnS core/shell NCs clearly confirm the diffusion of the Mn ions from the MnS core to the surface of the MnS/ZnS NCs during the above annealing process.

Figure 5 shows the temporal evolution of the PL intensity of MnS/ZnS core/shell NCs with a 3.7 ML ZnS shell (sample B) heated at various temperatures. As seen in Figure 5, no clear change in the PL intensity of Mn ions was observed in the sample annealed at a low temperature of 220 °C even for a long time. Similar results were also observed in samples A and C. This indicates that the diffusion of Mn ions cannot carry out below 220 °C. However, the PL was quenched significantly with increasing annealing temperature. The decrease of Mn ion PL intensity was observed at higher annealing temperatures. For example, at 300 °C for 140 min, the Mn ion PL decreased to 25% of the original PL QY, while at 250 °C for 140 min, it decreased to only 72%. Presumably, at higher temperature, the Mn ions diffuse more dramatically and move closer toward the surface of the lattice, resulting in more obvious PL decrease.[20] Therefore, the PL lifetime of Mn ions in the NCs after annealing for certain time will decrease as the annealing temperature increases. Figure 6 shows the change in the PL lifetime of Mn ions in the MnS/ZnS NCs annealed at various temperatures.

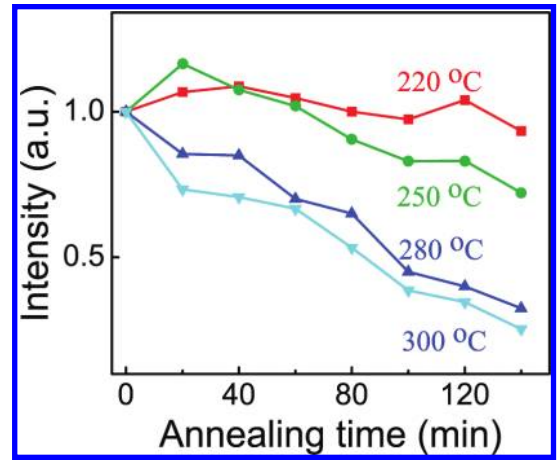

Figure 5. PL intensity of MnS/ZnS NCs with a 3.7 ML ZnS shell as a function of annealing time in the heat treatment temperature range of 220−300 °C.

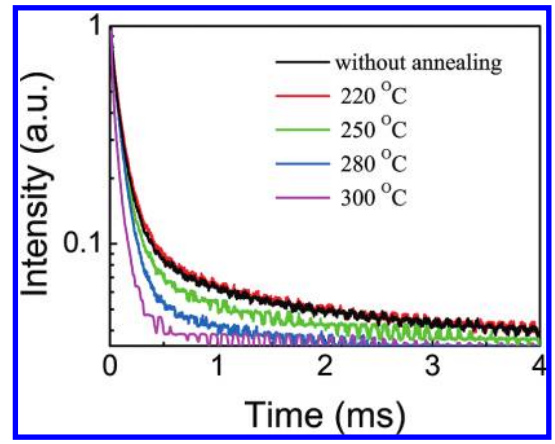

Figure 6. PL decay curves of MnS/ZnS NCs with a 3.7 ML ZnS shell heated at various temperatures for 80 min.

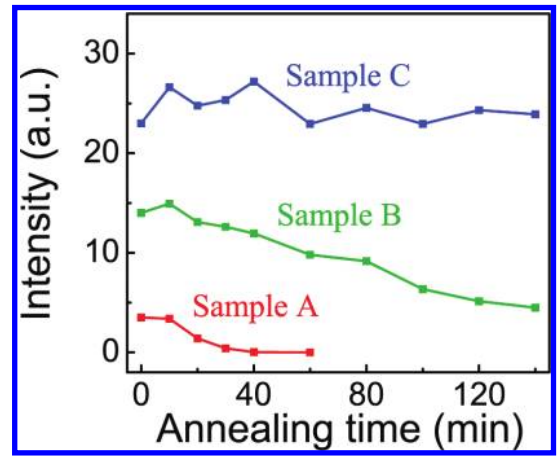

Figure 7. PL intensity of MnS/ZnS NCs with different shell thicknesses as a function of annealing time at a temperature of 280 °C.

The PL lifetime of Mn ions decreases monotonously from 1.71 to 0.95 ms with increasing annealing temperature from 220 to 300 °C for 80 min. Therefore, the decrease of PL intensity combining with the shortening of the PL lifetime is an indicator of the diffusion of Mn ions to the surface of NCs.

Figure 7 shows the PL intensity dependence of MnS/ZnS core/shell NCs with different shell thicknesses of 2.2, 3.7, and 5.0 MLs on the annealing time at a temperature of 280 °C. As obviously seen in Figure 7, the change in the PL intensity with increasing annealing time is found to be strongly dependent on

the shell thickness. For the MnS/ZnS NCs with a thin shell of 2.2 MLs (sample A), the PL intensity decreases rapidly and disappears completely after the thermal treatment for about 40 min, for the MnS/ZnS NCs with a shell of 3.7 MLs (sample B), the PL intensity slowly decreases with increasing annealing time during the entire annealing process of 140 min, while for MnS/ZnS NCs with a thick shell of 5.0 MLs (sample C), the PL intensity stays nearly constant. The above results imply that the dependence of the PL intensity on the annealing time is associated with the thickness of the ZnS shell. Peng's group also had observed the diffusion of Mn ions in MnSe/ZnSe NCs when they prepared the doped NCs using nucleation-doping strategy.[13] They suggested that the Mn ions might diffuse from the MnSe core into the overcoating ZnSe layer or move toward the surface during the overcoating of the thin ZnSe shell because some of the Mn ions are close to the NC surface.[13,20] This diffusion process could not occur for the NCs with a relatively thick ZnSe shell upon even thermal annealing up to 300 °C. Instead, such diffusion should occur during the overcoating process and seems to be limited to a relatively thin ZnSe shell.[13,20] Combined with our experiment results, we consider that there should be two different diffusion mechanisms during the growth process of the ZnS shell on the MnS core. The first one is the surface diffusion with a higher diffusion rate, which occurred at the initial growth process when a thin ZnS shell was grown on the MnS core as discussed above.[13,20] In the lifetime measurement for studying the diffusion, the longest lifetime of the Mn ion emission (1.35 ms) in sample A with a 2.2 ML ZnS shell is much shorter than the emission lifetime 1.8 ms of the single isolated Mn ions,[28,29] indicating that Mn ions have diffused to the surface of the NCs during the first overcoating processs.[17,28,29] Another one is the "lattice diffusion" with a rather slower diffusion rate, which occurred during additional overcoating of a ZnS passivating layer on the NCs, similar to the Mn ion diffusion in bulk CdTe.[18] Therefore, during the synthesis of the NCs with a thick ZnS shell, the diffusion of the Mn ions mainly occurs during the first overcoating process and can be negligible on the time scale of another overcoating process (only about 30 min at 250 °C).[18] This result is also consistent with the observation that for obtaining thermally more stable and more efficient MnSe/ZnSe emitters, the high temperature for the initial growth of the ZnSe layer is more important than a higher temperature for the subsequent overcoating.[13]

On the basis of the experiments discussed above, it is reasonable to hypothesize that the high-quality MnS/ZnS NCs can be realized by growing a thin ZnS layer on the MnS core at higher temperature in the initial growth stage and then overcoating a passivating ZnS layer on the NC surface. However, the result in our system is not consistent with the hypothesis. PL spectra of MnS/ZnS core/shell NCs with ZnS shells overcoated at temperatures of 200 °C (sample D), 250 °C (sample E), and 280 °C (sample F) are shown in Figure 8. The PL QYs of the Mn ions in the samples were estimated to be 42%, 26%, and 3%, respectively. It was noted that the PL QY of the Mn ions dramatically decreased with increasing the overcoating temperature, especially when the overcoating temperature increased to 280 °C. We monitored the growth process of MnS cores before the ZnS overcoating through TEM measurement. As shown in the inset of Figure 8, the MnS NCs were only about 1.8 nm in diameter when the reaction temperature increased to 200 °C, and then grew to 3.0 nm at the temperature of 250 °C. When the solution temperature further increased to 280 °C, serious NC Ostwald ripening was

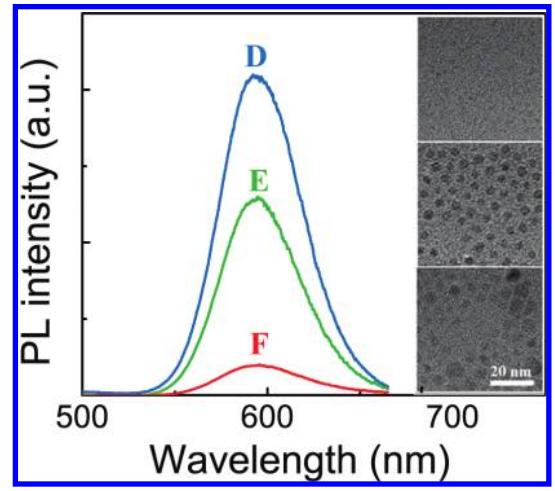

Figure 8. PL spectra of MnS/ZnS core/shell NCs with ZnS shells overcoated at temperatures of 200 °C (sample D), 250 °C (sample E), and 280 °C (sample F). The corresponding TEM images of the MnS cores before the ZnS overcoating are shown in the inset of this figure from top to bottom.

observed, causing a wide size distribution of the NCs in the range from 2.0 to 8.0 nm. It seems that the MnS cores are more unstable than MnSe cores synthesized at a temperature above 260 °C by Peng's group.[13] This might be due to the fact that the reactivity of ODES is higher than that of tributylphosphane selenium (TBPSe) precursor.[15,30] This makes us conclude that the small-sized MnS core is a key parameter for obtaining high-quality MnS/ZnS NCs, which is also confirmed by Peng's group.[13,15] A possible explanation is that the chemical potential of the NCs increases dramatically as the size decreases in the few nanometer range; thus. a small-sized core might be more suited for formation of a high-quality diffusion layer at the interface between the MnS core and ZnS shell in comparison to a large-sized MnS core.[13] Therefore, increasing the reaction temperature for the first overcoating process will initiate two competitive processes: increasing the PL QY by accelerating the diffusion of Mn ions from core to shell and decreasing the PL QY due to the increase of the MnS core size. To keep the small size of the MnS nanoclusters and not sacrifice the quality of the diffused interface layer, the synthesis procedure is modified as follows: first, growing a thin ZnS shell on a small-sized MnS core at low temperature, then annealing the resulting NCs for effective diffusion of Mn ions into the ZnS shell at higher temperature to form a ZnS:Mn diffusion layer, and finally overcoating a ZnS shell as a passivating layer at a certain temperature. We have reproducibly obtained highly efficient luminescent Mn-doped ZnS NCs with the maximum PL QY of 40−50% using this simple procedure.

Conclusions

In summary, the diffusion process of Mn ions in MnS/ZnS NCs annealed at various temperatures has been studied by steady-state and time-resolved PL spectroscopy. We demonstrate that Mn ions in MnS/ZnS NCs can diffuse from the MnS core to the surface of the NCs during prolonged annealing above temperatures of 220 °C via PL quenching of Mn ions. The diffusion layer of the MnS/ZnS core/shell NCs can be formed during the initial growth of the ZnS shell on the MnS core and an additional annealing process for the NCs with a thin ZnS shell, which is dependent on the overcoating temperature for the initial growth of ZnS shell as well as the size of the MnS core. Therefore, highly efficient luminescent Mn-doped ZnS (MnS/ZnS) NCs can be obtained by growing a

thin ZnS shell on a small-sized MnS core at low temperature, annealing the resulting NCs for effectively diffusing Mn ions into the ZnS shell at high temperature to form a ZnS:Mn diffusion layer, and overcoating a thicker ZnS shell as a passivating layer.[13,15,17,20,31]

Acknowledgment. This work was supported by the program of CAS Hundred Talents, the NSF of China (10874179, 60976049), and the Pre-Strategic Initiative of University of Tsukuba, Japan. The authors thank Professor Renguo Xie for his discussion in preparation of doped NCs.

References and Notes

(1) Bhargava, R. N.; Gallagher, D.; Hong, X.; Nurmikko, A. *Phys. Rev. Lett.* **1994**, *72*, 416.
(2) Norris, D. J.; Yao, N.; Charnock, F. T.; Kennedy, T. A. *Nano Lett.* **2001**, *1*, 3.
(3) Bol, A. A.; Meijerink, A. *J. Phys. Chem. B* **2001**, *105*, 10197.
(4) Karar, N.; Singh, F.; Mehta, B. R. *J. Appl. Phys.* **1999**, *95*, 656.
(5) Beaulac, R.; Archer, P. I.; Ochsenbein, S. T.; Gamelin, D. R. *Adv. Funct. Mater.* **2008**, *18*, 3873.
(6) Chen, L.; Zhang, J. H.; Luo, Y. S.; Lu, S. Z.; Wang, X. J. *Appl. Phys. Lett.* **2004**, *84*, 112.
(7) Cao, L. X.; Zhang, J. H.; Ren, S. L.; Huang, S. H. *Appl. Phys. Lett.* **2002**, *80*, 4300.
(8) Yang, H.; Holloway, P. H.; Ratna, B. B. *J. Appl. Phys.* **2003**, *93*, 586.
(9) Wood, V.; Halpert, J. E.; Panzer, M. J.; Bawendi, M. G.; Vladimir, B. *Nano Lett.* **2009**, *9*, 2367.
(10) Yang, X. H.; Xu, X. R. *Appl. Phys. Lett.* **2000**, *77*, 797.
(11) Zhuang, J. Q.; Zhang, X. D.; Wang, G.; Li, D. M.; Yang, W. S.; Li, T. J. *J. Mater. Chem.* **2003**, *13*, 1853.
(12) Pradhan, N.; Goorskey, D.; Thessing, J.; Peng, X. *J. Am. Chem. Soc.* **2005**, *127*, 17586.
(13) Pradhan, N.; Peng, X. *J. Am. Chem. Soc.* **2007**, *129*, 3339.
(14) Pradhan, N.; Battaglia, D. M.; Liu, Y.; Peng, X. *Nano Lett.* **2007**, *7*, 312.
(15) Zeng, R. S.; Rutherford, M; Xie, R. G.; Zou, B. S.; Peng, X. G. *Chem. Mater.* **2010**, *22*, 2107.
(16) Erwin, S. C.; Zu, L. J.; Haftel, M. I.; Efros, A. L.; Kennedy, T. A.; Norris, D. J. *Nature* **2005**, *436*, 91.
(17) Zheng, J. J.; Yuan, X.; Ikezawa, M.; Jing, P. T.; Liu, X. Y.; Zheng, Z. H.; Kong, X. G.; Zhao, J. L.; Masumoto, Y. *J. Phys. Chem. C* **2009**, *113*, 16969.
(18) Jamil, N. Y.; Shaw, D. *Semicond. Sci. Technol.* **1995**, *10*, 952.
(19) Dalpian, G. M.; Chelikowsky, J. R. *Phys. Rev. Lett.* **2006**, *96*, 226802.
(20) Chen, D. G.; Viswanatha, R. J.; Ong, G. L.; Xie, R. G.; Balasubramaninan, M.; Peng, X. G. *J. Am. Chem. Soc.* **2009**, *131*, 9333.
(21) Sandrine, I.; Philippe, G. S.; Benoit, M.; Benoit, D. *Phys. Rev. Lett.* **2007**, *99*, 265501.
(22) Shaw, D. J. *Introduction to Colloid and Surface Chemistry*; Butterworth-Heinemann: Oxford, U.K., 1992.
(23) Zu, L. J.; Norris, D. J.; Kennedy, T. A.; Erwin, S. C.; Efros, A. L. *Nano Lett.* **2006**, *6*, 334.
(24) Pradhan, N.; Reifsnyder, D.; Xie, R. G.; Aldana, J.; Peng, X. G. *J. Am. Chem. Soc.* **2007**, *129*, 9500.
(25) Jing, P. T.; Zheng, J. J.; Ikezawa, M.; Liu, X. Y.; Lv, S. Z.; Kong, X. G.; Zhao, J. L.; Masumoto, Y. *J. Phys. Chem. C* **2009**, *113*, 13545.
(26) Goede, O.; Heimbrodt, W. *Phys. Status Solidi B* **1988**, *146*, 11.
(27) Yang, Y. A.; Chen, O.; Angerhofer, A.; Cao, Y. *Chem.—Eur. J.* **2009**, *15*, 3186.
(28) Smith, B. A.; Zhang, J. Z.; Joly, A.; Liu, J. *Phys. Rev. B* **2000**, *62*, 2021.
(29) Huang, S. H.; You, F. T. *J. Lumin.* **2009**, *129*, 1692.
(30) Yang, Y. A.; Wu, H. M.; Williams, K. R.; Cao, Y. C. *Angew. Chem., Int. Ed.* **2005**, *44*, 6712.
(31) Xie, R. G.; Peng, X. G. *J. Am. Chem. Soc.* **2009**, *131*, 10645.

JP104513K